

# A Compact Apparatus for Muon Lifetime Measurement and Time Dilation Demonstration in the Undergraduate Laboratory

Thomas Coan,\* Tiankuan Liu,<sup>†</sup> and Jingbo Ye<sup>‡</sup>  
*Physics Department, Southern Methodist University, Dallas, TX 75275 USA*

We describe a compact apparatus that automatically measures the charge averaged lifetime of atmospheric muons in plastic scintillator using low-cost, low-power electronics and that measures the stopping rate of atmospheric muons as a function of altitude to demonstrate relativistic time dilation. The apparatus is designed for the advanced undergraduate physics laboratory and is suitable for field measurements.

## I. INTRODUCTION

Measurement of the mean lifetime of muons produced in Earth's atmosphere from collisions between cosmic rays and air nuclei is a common experiment<sup>1,2,3</sup> in advanced undergraduate physics laboratories. Typically, a single scintillating medium, massive enough to stop some useful fraction of the muons impinging on it, is viewed by one or two photomultiplier tubes (PMTs) that detect the pair of scintillation light flashes associated with the entry and subsequent decay of a stopped muon. Histogramming the time interval between the two flashes and then fitting the time distribution with an exponential function yield the mean muon lifetime. Various PMT readout and histogramming techniques have been implemented to produce the decay time histogram. However, such techniques tend to rely on relatively expensive and bulky electronic instrumentation (e.g., NIM and CAMAC-standard modules) and stand-alone multi-channel analyzers to generate the decay time histogram. We have developed fully equivalent readout instrumentation, based on a complex programmable logic device (CPLD<sup>4</sup>), that is compact ( $20 \times 25 \times 5 \text{ cm}^3$ ), low cost and low power ( $< 25 \text{ W}$ ). The readout instrumentation is easily interfaced to a laptop computer to display and fit the decay time histogram.

## II. DETECTOR AND READOUT ELECTRONICS

We use a standard detector configuration, with no attempt made to select only vertically traveling muons. A plastic scintillator in the shape of a right circular cylinder (15.2 cm diameter and 12.7 cm tall) is viewed by a single 10-stage, 51 mm diameter, bi-alkali photocathode PMT biased to nominal gain  $3 \times 10^5$  attached to one end. Both scintillator and PMT are wrapped carefully with aluminum foil and electrical tape to prevent light leaks. The PMT is biased using a compact, commercially available DC-DC converter<sup>5</sup> with negative high voltage (HV) applied to its photocathode. To mimic events where a muon enters, stops and then decays inside the scintillator, a blue light emitting diode (LED) is permanently inserted into a small hole drilled in one end of the scintillator. The LED can be driven by a transistorized pulser circuit that produces pairs of pulses at a nominal repetition rate of 100 Hz with an adjustable interpulse separation in a given pair from 300 ns to 30  $\mu\text{sec}$ . For robustness and portability, and so that no HV electrodes are exposed to students, the scintillator, PMT, HV circuit and pulser are all enclosed inside a black anodized aluminum tube 36 cm tall and 15.2 cm inner diameter. The cylinder is capped at both ends. Power to the HV supply and pulser circuitry is provided by a single multi-connector cable and the PMT signal is sent to the readout electronics module by a coaxial cable. Potentiometers installed in the cylinder cap allow student adjustment of the PMT HV and LED interpulse time separation. Provision is made to monitor the HV with a conventional voltmeter and output of the pulser circuitry is accessible by a coaxial connector on the cap. The mass of the overall detector is 5 kg.

The electronic circuitry to process PMT signals, perform timing, communicate with the computer, and provide power to the detector is mounted on one printed circuit board (PCB) located inside a single enclosure of volume  $20 \times 25 \times 5 \text{ cm}^3$ . A block diagram of this circuitry is shown in Fig. 1. Signals from the PMT anode are coupled by the coaxial cable to the input of a two-stage amplifier constructed from a fast current feedback amplifier<sup>6</sup>. A typical raw PMT signal amplitude for muon decay events is 100 mV into  $50 \Omega$  impedance. The amplifier output feeds a discriminator with adjustable threshold and TTL logic output. Students can monitor the amplifier and discriminator outputs via BNC connectors mounted on the front of the electronics enclosure.

The discriminator output signal is processed by a CPLD, mounted on a single PCB. A CPLD is a single, flexible integrated circuit (IC) comprised of thousands of usable logic gates that can implement a wide variety of digital logic functions. The chip includes programmable interconnections and multiple input/output (I/O) pins, and can be clocked at rates up to  $\sim 100 \text{ MHz}$ . Its behavior can be extensively and reliably simulated before its controlling

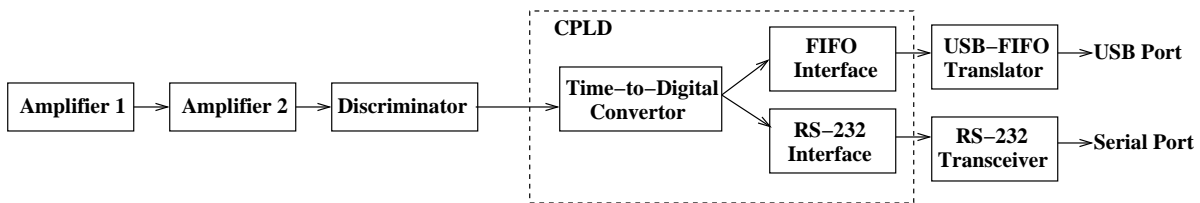


FIG. 1: Block diagram of the readout electronics showing the two-stage amplifier, discriminator, CPLD and I/O communications circuitry. Signals are processed from left to right.

program is downloaded into its electrically erasable programmable read only memory (EEPROM). Such ICs are reprogrammable and relatively cheap, typically costing a few tens of dollars, making the inexpensive implementation of a wide variety of digital logic signal processing circuitry practical.

The CPLD is programmed in a digital hardware description language (VHDL) to function primarily as a timer. A logical “yes” output from the discriminator, corresponding to an amplified PMT signal above threshold, causes either the CPLD to start recording clock cycles from the 50 MHz crystal oscillator that clocks it, or, if the CPLD had already started counting clock cycles, to stop counting. In this way, any amplified PMT signal above threshold can serve as a stop or start timing signal. The CPLD is also programmed to reset itself if a second “yes” does not occur within  $20\ \mu\text{sec}$  of the first one. This simple logic scheme corresponds to our desired event scenario where we have a flash of scintillator light corresponding to a muon entering and stopping in the scintillator, and a second flash occurring when the stopped muon decays.

The CPLD formats data in a simple fashion. For successive PMT signals above threshold and within the  $20\ \mu\text{s}$  timing window, the time difference, in integral units of 50 MHz clock cycles, between these two signals is recorded. Data of this type is ultimately histogrammed and fit to an exponential curve by the laptop software to extract the muon lifetime. For cases when there are no signal pairs within the timing window, the CPLD merely records the integer 1000, corresponding to the number of clock cycles in our timing window. All data are subsequently sent to the laptop through either a serial or USB port.

The CPLD I/O circuitry (see Fig 1) has two physical ports to simplify interfacing to laptop computers. One port is a standard serial port that follows the RS-232 protocol and that relies on a dedicated RS-232 transceiver chip to shift RS-232 standard voltage levels to low voltage TTL levels to communicate with the RS-232 interface module resident in the CPLD. The data transmission rate between CPLD and laptop is 115 kbits/s. The other port adheres to the USB 1.1 protocol and relies on a USB-FIFO (“first in, first out”) translator chip to communicate with the FIFO interface module within the CPLD. Data transmission rates in this case are 2.4 Mbits/s.

Overall power consumption of the electronics module is less than 25 W, sufficiently low that it can be powered in the field from an automobile cigarette lighter.

### III. DATA DISPLAY SOFTWARE

The laptop-resident software that displays and curve fits the decay time histogram is written in the Tcl/Tk scripting language, an open source language that permits easy implementation of graphical user interfaces and that is compatible with Unix, Microsoft Windows and Apple Macintosh operating systems. The laptop continuously examines its own I/O port buffers for the presence of any data that the CPLD has sent it. Any data consistent with PMT pulse pairs within the timing window has the corresponding pulse separation time entered into a decay time histogram. Data not corresponding to pulse pairs is used to update various rate meters monitoring the frequency of PMT signals above threshold. All data is then slightly reformatted to include the absolute time in seconds when it was examined by the laptop before being written to disk in ASCII format for easy human interpretation and exporting to student written data analysis software routines. The histogram and rate meters are displayed in real time for student observation.

The laptop software has provision for simulating muon decay by randomly generating times according to an exponential distribution with a user selectable lifetime. This permits students to practice their curve fitting and lifetime extracting software routines on large simulated data sets.

### IV. MEAN MUON LIFETIME

A decay time histogram for muons stopping in our detector formed by histogramming the time between two successive scintillator flashes within our  $20\ \mu\text{s}$  timing window is shown in Fig. 2. Dots with crosses are data and the line

is a fit to the data. This histogram contains 28,963 events collected over 480 hours of running and contains  $\mu^+$  and  $\mu^-$  decays as well as background. The data is fit to the functional form  $\dot{N}(t) = P_1 P_2 \exp(-P_2 t) + P_3$ , characteristic of radioactive decay with background. Here  $\dot{N}(t)$  represents the observed number of decays per unit time at time  $t$  and the quantities  $P_1$ ,  $P_2^{-1}$  and  $P_3$  are constants extracted from the fit and represent an overall normalization constant, the muon lifetime and the background level, respectively. These values are shown in the box in the upper right-hand corner of Fig. 2. The quality of the fit is indicated by the low  $\chi^2$  per degree-of-freedom ( $\chi^2/\text{d.o.f.} = 73/55$ ). The fit was done with PAW, a freely available<sup>7</sup> fitting and plotting software package. Other fitting packages return similar results. Due to the properties of an exponential function, it is irrelevant that the muons whose decays we observe are undetected when born outside the detector.

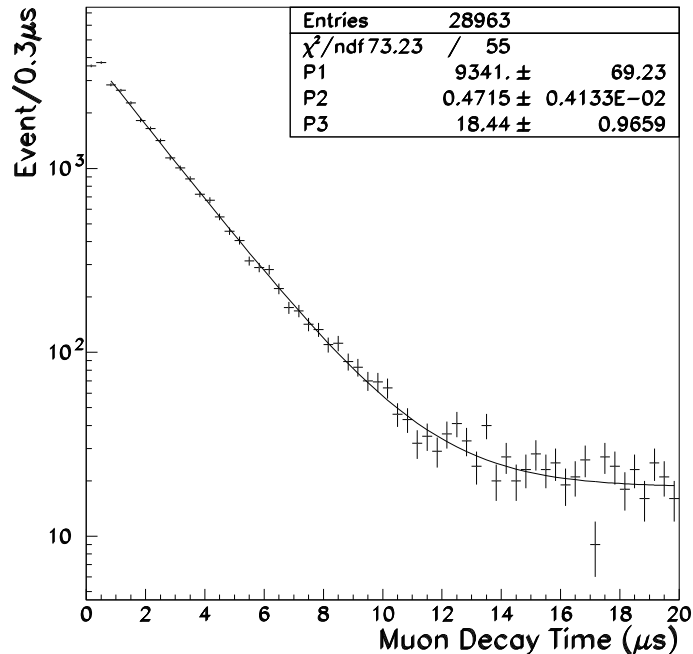


FIG. 2: Decay time histogram for 28,963 events collected over 480 hrs. The dots with error bars are data and the line is a fit to the data with the three-parameter function  $f(t) = P_1 P_2 \exp(-P_2 t) + P_3$ . The values for the fit parameters plus the  $\chi^2$  per degree-of-freedom are shown in the upper right hand corner.

The extracted value of the mean muon lifetime  $\tau = P_2^{-1} = 2.12 \pm 0.02 \mu\text{s}$  (statistical error only) is less than the free space value  $\tau_\mu = 2.19703 \pm 0.00004 \mu\text{s}$  due to the non-negligible probability that a  $\mu^-$ , but not a  $\mu^+$ , will be captured into the K-shell of a scintillator carbon atom and then be absorbed by its nucleus<sup>8</sup>. (The probability that a stopped  $\mu^-$  will be absorbed by a target atom of atomic number  $Z$  is proportional to  $Z^4$ .)

The extracted background rate of fake muon decays is inferred from the value of  $P_3$  and the 480 hr running time, and corresponds to 0.6 mHz. This rate of two PMT signals in coincidence is consistent with the observed rate of single PMT signals above threshold ( $\sim 6$  Hz) and our  $20 \mu\text{s}$  timing window. For comparison, the fitted rate of muon decays in the scintillator is 17 mHz ( $\sim 1 \text{ min}^{-1}$ ).

From the charge averaged lifetime of muons in what is essentially a carbon target (the ratio of hydrogen to carbon in plastic scintillator is 1:1), and the lifetime of  $\mu^-$  in carbon<sup>9</sup>, it is straightforward<sup>10</sup> to measure the charge ratio abundance  $\rho = N(\mu^+)/N(\mu^-)$  of low-energy ( $E \lesssim 200 \text{ MeV}$ ) muons at sea-level. For example, from our measured lifetime, we find  $\rho = 1.08 \pm 0.01$  (statistical error only), averaged over the angular acceptance of the detector, a value consistent with the diminishing trend<sup>11</sup> for  $\rho$  as the muon momentum approaches zero.

## V. DEMONSTRATION OF RELATIVISTIC TIME DILATION

The stopping rate of muons in the detector as a function of altitude above sea level can be used to demonstrate relativistic time dilation. Although the detector design is non-optimal for this demonstration since it is sensitive

to muons with a range of velocities as well as non-vertical trajectories, it has the advantage that no bulky velocity selecting absorbers or additional trajectory defining scintillators<sup>12</sup> are required. The idea is simple. The total number of stopped muons in the detector in some fixed time interval and at some fixed altitude above sea level (a.s.l.) is measured from the decay time histogram. A lower altitude is selected and predictions made for the new stopping rate that do and do not include the time dilation effect of special relativity. Measurement then discriminates between the two predictions.

To make the comparison between the competing assumptions meaningful, the effects of the energy loss of a muon as it descends in the atmosphere as well as the shape of the sub-GeV/c muon momentum spectrum<sup>13</sup> near sea-level should be included. The first effect tends to increase the transit time of the muon from one altitude to another and the other tends to over emphasize the effects of time dilation.

The transit time  $t'$  measured in the muon's rest frame as it descends vertically in the atmosphere from a height  $H$  down to sea-level is given by

$$t' = \int_H^0 \frac{dh}{c\beta(h)\gamma(h)} \quad (1)$$

where  $\beta$  and  $\gamma$  have their normal relativistic meanings,  $dh$  is a differential element of pathlength and  $c$  is the speed of light. All quantities on the right-hand side of Eq. (1) are measured in the detector rest frame. As the muon descends it loses energy in a manner described by the Bethe-Bloch equation<sup>14</sup> so the integral can be evaluated numerically if great precision is desired. Instead, we use the common approximation that a singly-charged relativistic particle loses energy by ionization and excitation of the medium it traverses with a magnitude  $dE/dx = 2 \text{ MeV g}^{-1} \text{ cm}^2$  ( $\equiv S_0$ ). Eq. (1) becomes

$$t' \simeq \frac{mc}{\rho S_0} \int_{\gamma_2}^{\gamma_1} \frac{d\gamma}{\sqrt{\gamma^2 - 1}} \quad (2)$$

Here,  $\gamma_1$  is the muon's Lorentz factor at height  $H$ ,  $\gamma_2$  is its Lorentz factor just before it enters the sea level scintillator,  $m$  is the muon mass and  $\rho$  denotes the pathlength-averaged mass density of the atmosphere. We take  $\gamma_2 \simeq 1.5$  since we want muons that stop in the scintillator and assume, consistent with our detector geometry, that stopped muons travel an average distance  $s = 10 \text{ g/cm}^2$  in the scintillator. (See muon range-momentum graphs from the Particle Data Group<sup>15</sup> for correlating a muon's range with its momentum.) The appropriate value of  $\gamma_1$  depends on the height  $H$  where we take our upper measurement and is computed from the energy  $E_1$  a muon has at that height if it is to arrive at the sea-level detector with  $\gamma_2 = 1.5$  (corresponding to energy  $E_2 = 160 \text{ MeV}$ ). Clearly, if a muon loses energy  $\Delta E$  in traversing a vertical distance  $H$ , then  $E_1 = \Delta E + 160 \text{ MeV}$ . The quantity  $\Delta E$  can be computed from the Bethe-Bloch equation or estimated from the above rule-of-thumb for minimum ionizing particles and properties of the standard atmosphere.

Since the time dilation demonstration relies on stopping muons in the detector, we must account for the fact that muons that eventually stop in the lower detector have, at the position of the upper detector, an energy that is greater than those muons that would be stopped in the upper detector. Since the momentum spectrum of sub-GeV muons near sea-level is not flat, but peaks at muon momentum  $p_\mu \sim 500 \text{ MeV}/c$ , we correct for this affect so that the effective flux of incident muons is appropriately normalized. (This is easy to see if you assume muons don't decay at all and only lose energy in the atmosphere as they descend.) We do this by measuring the ratio of stopping rates at a pair of altitudes to determine a single scaling factor that we can apply to other pairs of altitudes.

To illustrate the procedure, we measure the muon stopping rate at two different elevations ( $\Delta h = 3,000 \text{ m}$  between Taos, NM and Dallas, TX) and compute the ratio  $R_{\text{obs}}$  of observed stopping rates ( $R_{\text{obs}}(\text{Dallas/Taos}) = 0.41 \pm 0.05$ .) The transit time  $t'$  in the muon's rest frame for vertical trajectories between the two elevations is computed using Eq. 2 and yields  $t' = 1.32\tau_\mu$ . This corresponds to a naive theoretical stopping rate ratio  $R = \exp(-t'/\tau_\mu) = 0.267$ . The double ratio  $R_0 = R_{\text{obs}}/R = 1.5 \pm 0.2$  is then interpreted as a correction factor for the shape of the muon momentum spectrum. Note that this same correction tends to account for muons with non-vertical trajectories that stop in the detector. These slanting muons with a projection onto the vertical axis of distance  $H$  travel further in the atmosphere and hence start with more energy than their purely vertical counterparts.

To verify that the procedure is sensible, we choose a new elevation ( $H = 2133 \text{ m a.s.l.}$  at Los Alamos, NM), compute the transit time  $t' = 1.06\tau_\mu$  and the expected stopping rate ratio (Dallas/Los Alamos)  $R_{\text{thy}} = R_0 \exp(-t'/\tau_\mu) = 0.52 \pm 0.06$ . The observed ratio  $R_{\text{obs}} = 0.56 \pm 0.01$ , showing good agreement. Table I summarizes relevant measurements and lists in the third column calculated proper transit times for vertical muon trajectories, in units of the proper muon lifetime  $\tau_\mu$  and relative to Dallas' elevation.

To compare the stopping rate measurements with the competing assumption that there is no time dilation effect ("ntd"), we proceed as before except we calculate the transit time in the detector rest frame and we assume all muons

TABLE I: Muon Stopping Rate Measurements and Calculated Proper Transit Times

Elevation (meters a.s.l.)	Observed Stopping Rate ( $\text{min}^{-1}$ )	Proper transit time ( $\tau_\mu$ )
146	$1.24 \pm 0.01$	—
2133	$2.21 \pm 0.05$	1.06
3154	$3.00 \pm 0.34$	1.32

travel at the speed of light so as to *minimize* the effect of time dilation. For the case of transit between Los Alamos and Dallas, the transit time  $t_{\text{ntd}}$  in the detector rest frame is  $t_{\text{ntd}} = 6.62 \mu\text{s}$ , implying an expected stopping rate ratio  $R_{\text{ntd}} = R_0 \exp(-t/\tau) = 0.08 \pm 0.01$ , a result strongly disfavored by observation.

## VI. SUMMARY

We have designed a compact and low-cost apparatus for measuring the mean muon lifetime and for demonstrating relativistic time dilation suitable for undergraduate teaching. An electronics schematic and Tcl/Tk data acquisition/display software are available upon request.

## Acknowledgments

The technical assistance of H. van Hecke and L. Lu is greatly appreciated, as well as the financial support of the Lightner-Sams foundation.

- 
- \* Electronic address: coan@mail.physics.smu.edu
  - † Electronic address: liu@mail.physics.smu.edu
  - ‡ Electronic address: yejb@mail.physics.smu.edu
  - <sup>1</sup> R.E. Hall, D.A. Lind and R.A. Ristinen, *Am. J. Phys.* **38**, 1196 (1970).
  - <sup>2</sup> A. Owens and A.E. Macgregor, *Am. J. Phys.* **46**, 859 (1978).
  - <sup>3</sup> R.J. Lewis, *Am. J. Phys.* **50**, 894 (1981).
  - <sup>4</sup> Part EPM7128BTC100-10, Altera Corp., [www.altera.com](http://www.altera.com).
  - <sup>5</sup> Model G12, EMCO High Voltage Corp., [www.emcohighvoltage.com](http://www.emcohighvoltage.com).
  - <sup>6</sup> Part AD8004AR-14, Analog Devices, [www.analog.com](http://www.analog.com).
  - <sup>7</sup> PAW graphing and plotting package, <http://wwwasd.web.cern.ch/wwasd/paw/>.
  - <sup>8</sup> T. Ward *et al.*, *Am. J. Phys.* **53**, 542 (1985).
  - <sup>9</sup> R.A. Reiter *et al.*, *Phys. Rev. Lett.* **5**, 22 (1960).
  - <sup>10</sup> B. Rossi, *High-Energy Particles* (McGraw-Hill, New York, 1952).
  - <sup>11</sup> I.M. Brancus *et al.*, *28th International Cosmic Ray Conference* (Tsukuba, Japan, 2003).
  - <sup>12</sup> N. Easwar and D.A. MacIntire, *Am. J. Phys.* **59**, 589 (1991).
  - <sup>13</sup> P.K.F. Greider, *Cosmic Rays at Earth* (Elsevier, Amsterdam, 2001), p399.
  - <sup>14</sup> W.R. Leo, *Techniques for Nuclear and Particle Physics Experiments* (Springer-Verlag, 1994).
  - <sup>15</sup> *The Review of Particle Physics*, Particle Data Group, <http://pdg.lbl.gov>.